International Journal of Fracture **101**: L9–L14, 2000.

A COMPUTATIONAL MODEL FOR INTERFACIAL DAMAGE THROUGH MICROSTRUCTURAL COHESIVE ZONE RELAXATION

Tarek I. Zohdi
Institute for Structural Mechanics and Computational Mechanics
Appelstrasse 9A, 30167 Hannover, Germany
zohdi@ibnm.uni-hannover.de fax. 49-(0511)-762-5496

Peter Wriggers
Institute for Structural Mechanics and Computational Mechanics
Appelstrasse 9A, 30167 Hannover, Germany
wriggers@ibnm.uni-hannover.de fax. 49-(0511)-762-5496

Abstract. A model introducing cohesive zones around material interfaces to simulate interfacial damage in microheterogeneous materials is developed. The material behavior within the cohesive zones is unknown a-priori, and is weakened, or "relaxed", on the continuum level from an initially undamaged state, by a reduction of the spatially variable elasticity tensor's eigenvalues. This reduction is initiated if constraints placed on the microstress fields, for example critical levels of pressure or deviatoric stresses, are violated. Outside of the cohesive zones the material is unaltered. Numerical computations are performed, employing the finite element method, to illustrate the approach in three dimensional applications.

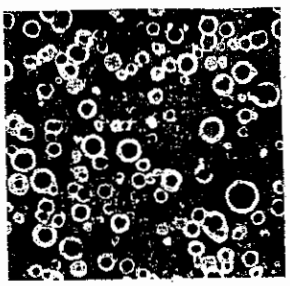

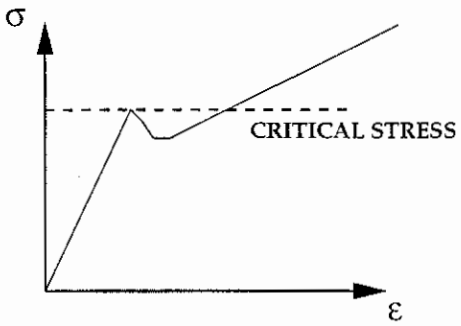

Figure 1: An example of ductile iron consisting of embedded graphite nodules (spherulites) encased in envelopes of free ferrite in a matrix of pearlite, magnified 100 × (Metals Handbook (1978)). Qualitatively observed overall response of materials undergoing interfacial damage.

1. Introduction. Due to their versatility and advantageous properties, tailored materials with heterogeneous microstructure have become widely used in structural applications. For a structural analyst, the quantities of interest

are usually related to the overall design of a mechanical response of an assemblage of material, for example, several particles suspended in a binding matrix material (Figure 1). A primary concern in the use of such materials are losses due to microstructural damage resulting from highly distorted microfields arising from property mismatches within the material microstructure. In particular, interfacial degradation is an important issue. Clearly, if the binding material becomes damaged, then virtually all of the advantageous aggregate properties are lost. There exist no analytical solutions for finite domains with multiple debonding/damaged interfaces. Simulation of the progressive damage of material interfaces in large statistically representative samples of materials requires approaches amenable to rapid computation. One approach is to employ cohesive zone models, which have recently received a great deal of attention in the literature, although their use over the last 30 years, in one way or the other, has been widespread. Cohesive zone models have physical motivation, since observations have shown that a thin interface layer can form that differs structurally, and, consequently, mechanically from the materials on either side of the interface (Figure 1). The usual application of cohesive zone approaches is to represent imperfect bonding by a thin elastic film having shear stress that is dependent on the relative displacement at the interface. This approach has been adopted in numerical simulations designed to study failure of the interface. For example, many studies have employed special finite elements with triggered damage mechanisms at predetermined stress levels such as in Needleman (1987, 1992) or recently in Ortiz and Pandolfi (1999).

In this paper a model introducing cohesive zones around material interfaces to simulate interfacial damage in microheterogeneous materials is developed. In the approach the material behavior within the cohesive zones is unknown a-priori, and "relaxes" (softens) on the continuum level from an undamaged state, by a reduction of the elasticity tensor's eigenvalues. This is initiated if constraints placed on components of the maximum attainable stress are violated (Figure 1). Outside of the cohesive zones, the material is unaltered. Numerical computations are performed to illustrate the applicability of the approach to full three dimensional cohesive zone models.

2. Effects of material relaxation. We consider a structure which occupies a bounded domain Ω with a boundary denoted $\partial\Omega$. The body is in static equilibrium under the action of body forces, $\boldsymbol{f}$, and surface tractions, $\boldsymbol{t}$. The boundary $\overline{\partial\Omega} = \overline{\Gamma_u \cup \Gamma_t}$ consists of a part Γ_u and a part Γ_t on which displacements and tractions are respectively prescribed. The undamaged (virgin) mechanical properties of the heterogeneous material are characterized

(pointwise) by the elasticity tensor $\mathbb{E}$ which is assumed to satisfy standard symmetry and positive-definiteness conditions. We denote $\boldsymbol{u}$ as the "unrelaxed" (undamaged) solution field of the following variational boundary value problem:

$$\boxed{\begin{array}{l}\text{Find } \boldsymbol{u}, \boldsymbol{u}|_{\Gamma_u} = \boldsymbol{d}, \text{ such that} \\ \displaystyle\int_\Omega \nabla \boldsymbol{v} : \mathbb{E} : \nabla \boldsymbol{u}\, d\boldsymbol{x} = \int_\Omega \boldsymbol{f} \cdot \boldsymbol{v}\, d\boldsymbol{x} + \int_{\Gamma_t} \boldsymbol{t} \cdot \boldsymbol{v}\, ds \quad \forall \boldsymbol{v}, \boldsymbol{v}|_{\Gamma_u} = \boldsymbol{0}.\end{array}} \tag{1}$$

This formulation contains no microscopic damage or what we will refer to as "relaxation" effects. To describe losses of strength in the material on the microscopic level, we construct a relaxed solution, $\boldsymbol{u}_{\text{rel}}$, that is generated by a weakened material modulus, $\mathbb{E}_{\text{rel}} \leq \mathbb{E}$. The notation $\mathbb{E}_{\text{rel}} \leq \mathbb{E}$ means that the eigenvalues of $\mathbb{E} - \mathbb{E}_{\text{rel}}$ are nonnegative. The corresponding variational boundary value problem governing the relaxed solution is:

$$\boxed{\begin{array}{l}\text{Find } \boldsymbol{u}_{\text{rel}}, \boldsymbol{u}_{\text{rel}}|_{\Gamma_u} = \boldsymbol{d}, \text{ such that} \\ \displaystyle\int_\Omega \nabla \boldsymbol{v} : \mathbb{E}_{\text{rel}} : \nabla \boldsymbol{u}_{\text{rel}}\, d\boldsymbol{x} = \int_\Omega \boldsymbol{f} \cdot \boldsymbol{v}\, d\boldsymbol{x} + \int_{\Gamma_t} \boldsymbol{t} \cdot \boldsymbol{v}\, ds \quad \forall \boldsymbol{v}, \boldsymbol{v}|_{\Gamma_u} = \boldsymbol{0} \\ \text{If } \mathcal{M} < \mathcal{K} \text{ then } \mathbb{E}_{\text{rel}} = \mathbb{E} \quad \text{(no relaxation)} \\ \text{If } \mathcal{M} = \mathcal{K} \text{ then } \boldsymbol{0} < \mathbb{E}_{\text{rel}} \leq \mathbb{E} \quad \text{(relaxation)}\end{array}} \tag{2}$$

$\mathcal{M} = \mathcal{M}(\mathbb{E}_{\text{rel}}, \boldsymbol{u}_{\text{rel}}, \alpha)$ and $\mathcal{K} = \mathcal{K}(\mathbb{E}_{\text{rel}}, \boldsymbol{u}_{\text{rel}}, \alpha)$ respectively serve as a measure of, and constraint on, selected internal fields of interest to the analyst. Clearly, a sufficient way to meet our physical restrictions, is to force the eigenvalues of $\mathbb{E}_{\text{rel}}$ to decrease at a location where failure occurs, and to remain constant otherwise. In the simplest case, one can define a spatially varying scalar function, α, such that $\mathbb{E}_{\text{rel}} = \alpha \mathbb{E}$ with $0 < \alpha \leq 1$. The scalar function α takes on different values throughout the body, which are dictated by the solution to the relaxed boundary value problem. The functions $\mathcal{M}$ and $\mathcal{K}$ could be scalar, vector, or tensor valued. When the material is directionally independent (2 free constants), we have $\mathbb{E} : \boldsymbol{\epsilon} = 3\kappa \frac{tr\boldsymbol{\epsilon}}{3} \boldsymbol{I} + 2\mu \boldsymbol{\epsilon}'$, where $tr\boldsymbol{\epsilon} = \epsilon_{ii}$ and $\boldsymbol{\epsilon}' = \boldsymbol{\epsilon} - \frac{1}{3}(tr\boldsymbol{\epsilon})\boldsymbol{I}$. The eigenvalues of an isotropic elasticity tensor are $(3\kappa, 2\mu, 2\mu, \mu, \mu, \mu)$. Therefore, we must have $\alpha\kappa > 0$ and $\alpha\mu > 0$ to retain positive definiteness of $\mathbb{E}$. For the constraints, for example, one could use a stress level, $\mathcal{M} = ||\boldsymbol{\sigma}_{rel}|| \leq ||\boldsymbol{\sigma}^{\text{crit}}|| = \mathcal{K}$. An important observation is that one can restrict the relaxation to "zones of interest" as in Figure 2. In this paper the zones of interest, the cohesive zones, are depicted in Figure 2.

3 Computational procedure. The values of α are dictated by the fact that the solution $\boldsymbol{u}_{\text{rel}}$ must satisfy the equations of equilibrium, and simultaneously the constraints. Algorithmically, when the constraint is violated during loading we must enforce

$$\Phi(\alpha) \stackrel{\text{def}}{=} \mathcal{M}(\boldsymbol{\sigma}(\alpha)) - \mathcal{K}(\alpha) = 0 \tag{3}$$

where $\mathcal{M}(\boldsymbol{\sigma}(\alpha)) \stackrel{\text{def}}{=} g : g$ and $\mathcal{K}(\alpha) \stackrel{\text{def}}{=} (\Phi^{lim} + (\Phi^{crit} - \Phi^{lim})\alpha^P)^2$, $g(\boldsymbol{\sigma}) \stackrel{\text{def}}{=} w_1 \frac{tr\boldsymbol{\sigma}}{3}\boldsymbol{I} + w_2(\boldsymbol{\sigma} - \frac{tr\boldsymbol{\sigma}}{3}\boldsymbol{I})$, $g(\boldsymbol{\sigma}) : g(\boldsymbol{\sigma}) = w_1^2 3(\frac{tr\boldsymbol{\sigma}}{3})^2 + w_2^2 \boldsymbol{\sigma}' : \boldsymbol{\sigma}'$, and where w_1 and w_2 are positive weights which reflect the type of damage, hydrostatic and/or deviatoric, to be expected and where Φ^{crit} and Φ^{lim} are specified material-dependent functions, i.e. critical and limit levels of stress. The condition in equation (3) can be enforced with a relatively standard implicit global-local Newton "tangent-stiffness" procedure for problems with constraints. See, for example, Wriggers (1995).

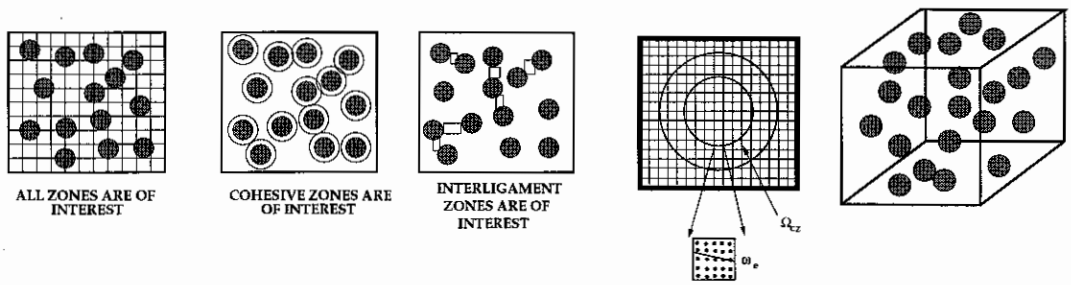

Figure 2: Restricted relaxation to cohesive zones. Finite element representation. 20 randomly distributed Boron spheres in an Aluminum matrix.

4 Three dimensional cohesive zone simulations. To model three dimensional cohesive zone requires the restriction of the relaxation to cohesive zones encompassing the particles (Figure 2). Outside of the cohesive zone the material is unrelaxed. The domain of a cohesive zone, Ω_{CZ}, is defined via, $\Omega_{CZ} \stackrel{\text{def}}{=} \Omega_{P+\delta P} - \Omega_P$, where $\Omega_{P+\delta P}$ is a dilatated form of Ω_P (Figure 2). To increase the resolution of the internal geometry, we apply a "2/5" Gauss rule, i.e. a $2 \times 2 \times 2$ Gauss rule if there is no discontinuity in the element, and a $5 \times 5 \times 5$ rule if there is a discontinuity. Numerical studies of such "over-sampling" approaches have been presented in Zohdi and Wriggers [6]. The microstructure was produced by randomly distributing 20 equal sized boron particles occupying 18 % of the volume of the aluminum-matrix box. If the

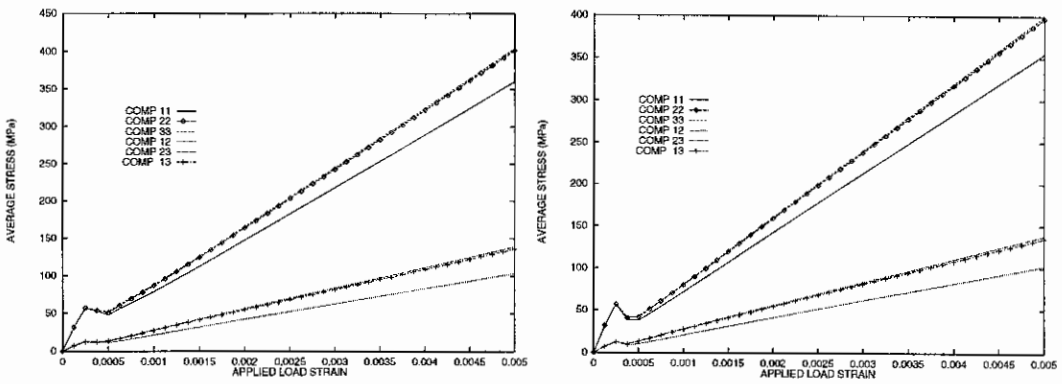

Figure 3: Overall responses. Left: $P = 0.1$. Right: $P = 0.95$.

constraint equation (3) was violated for $\boldsymbol{x} \in \Omega_{CZ}$ then relaxation was initiated. The cohesive zone thicknesses were taken to be kr, $k = 0.3$, where r is the radius of the particle, consistent with observed thicknesses, for example those in Figure 1. The load step size was set to 40 displacement controlled load increments to guide the following displacement controlled boundary loading history, $\boldsymbol{u}|_{\partial\Omega} = \mathcal{E}^{begin} \cdot \boldsymbol{x} \rightarrow \mathcal{E}^{final} \cdot \boldsymbol{x}$, where $\mathcal{E}$ is an applied second order strain tensor with components $\mathcal{E}_{ij}$. We selected $\mathcal{E}_{ij}^{begin} = 0.00$ and $\mathcal{E}_{ij}^{final} = 0.005$. The constraint constants were selected to be $\Phi^{crit} \stackrel{\text{def}}{=} \sqrt{w_1^2(\Phi_{dil}^{crit})^2 + w_2^2(\Phi_{dev}^{crit})^2}$ and $\Phi^{lim} = \beta\% \times \Phi^{crit}$, where the values entering the constraint function for the cohesive zones ($\mathcal{K}(\alpha)$) were those of the Aluminum: $(\kappa, \mu, \Phi_{dil}^{crit}, \Phi_{dev}^{crit}) = (77.9\,GPa, 24.9\,GPa, 40\,MPa, 80\,MPa)$. We chose $\beta\% = 50\%$. The material values of the Boron were Boron $(\kappa, \mu) = (230\,GPa, 172\,GPa)$. The finite element meshes were repeatedly refined until no changes in the macroscopic responses occurred. Approximately at a $24 \times 24 \times 24$ trilinear brick mesh density (2344 numerical degrees of freedom *per particle*) the results stabilized. Figure 3 illustrates typical responses. As intuitively expected, the exponent of relaxation was increased, the weakening in strength for both the dilatational and shear components, in the initial damage response is observed. An initially linear response occurs, relatively stiff due to the unrelaxed interface, i.e. the "bond" is still intact. There is then a transition period where the cohesive zone relaxes, and after a few increments, a new linear elastic response, essentially that of the aluminum, appears. The boron plays no role after this point. Such curves are typical for composites undergoing interfacial damage. It is important to note that the nonmonotonicity is to be expected since $\boldsymbol{\sigma} = \alpha \mathbb{E} : \boldsymbol{\epsilon} \Rightarrow d\boldsymbol{\sigma} = d\alpha \mathbb{E} : \boldsymbol{\epsilon} + \alpha \mathbb{E} : d\boldsymbol{\epsilon} \stackrel{\text{def}}{=} \mathbb{E}^{\text{TAN}} : d\boldsymbol{\epsilon}$, $d\alpha \leq 0$. In other

words, the tangent stiffness is not necessarily positive definite throughout the loading. An important observation is that texture of the responses develops with increasing loads. In other words, the responses like $\langle\sigma_{11}\rangle_\Omega$ vs. $\langle\epsilon_{11}\rangle_\Omega$ and $\langle\sigma_{22}\rangle_\Omega$ vs. $\langle\epsilon_{22}\rangle_\Omega$, which would be identical if the macroscopic response was perfectly isotropic, began to deviate. This is attributed to the inhomogeneous relaxation spreading nonuniformly through the structure. In general, the approach can be considered as an optimization algorithm, whereby the material in specified zones of interest must be adjusted ("optimized") to meet a desired criteria. A more mathematically detailed presentation of the model, can be found in Zohdi and Wriggers [7].

REFERENCES

1. Metals Handbook (1978). *Failure Analysis and Prevention.* The American Society for Metals. Volume 9, 88.

2. Needleman, A. (1987). A continuum model for void nucleation by inclusion debonding. *J. Appl. Mech.* **54**, 525-531.

3. Needleman, A. (1992). Micromechanical modeling of interfacial decohesion. *Ultramicroscopy.* **40**, 203-214.

4. Ortiz, M. and Pandolfi. A. (1999). Finite deformation irreversible cohesive elements for three-dimensional crack-propagation analysis. *The International Journal of Numerical Methods in Engineering.* **44**, 1267-1282.

5. Wriggers, P. (1995). Finite element algorithms for contact problems. *Archives of Computational Methods in Engineering.* **2**, **4**, 1-49.

6. Zohdi, T. I. and Wriggers, P. (under review). Some aspects of the computational testing of the mechanical properties of microheterogeneous material samples.

7. Zohdi, T. I. and Wriggers, P. (under review). A model for simulating the deterioration of structural-scale material responses of microheterogeneous solids.